Thin Solid Films 519 (2011) 4329–4333

Contents lists available at ScienceDirect

Thin Solid Films

journal homepage: www.elsevier.com/locate/tsf

Extraordinary Hall effect in nanoscale nickel films

V. Volkov, V. Levashov *, V. Matveev, L. Matveeva, I. Khodos, Yu Kasumov

Institute of Microelectronics Technology and High Purity Materials, Russian Academy of Sciences, 6, Institutskaya Street, Chernogolovka, Moscow Region, 142432, Russia

ARTICLE INFO

Article history:
Received 10 September 2010
Received in revised form 27 January 2011
Accepted 31 January 2011
Available online 10 March 2011

Keywords:
Nickel
Hall effect
Electron-beam evaporation
Sputtering
Thin films
Hall resistance
Extraordinary Hall coefficients

ABSTRACT

The extraordinary Hall effect was studied in 1 to 10nm thick nickel films prepared by radio-frequency diode sputtering (plasma) and electron-beam evaporation of Ni. The Hall resistance, R_H, does not reach saturation in fields up to 0.5 T in films that are not uniform while for uniform films, R_H saturates at 0.3 T. The films prepared by plasma sputtering showed a jump-like behavior of the extraordinary Hall coefficient, R_S, that is due to the presence of two phases—tetragonal (nonmagnetic) and face-centered cubic(fcc) (magnetic)—in the initial growth stage and subsequent phase transition of the tetragonal lattice to fcc at a film thickness of about 4 nm around which the extraordinary Hall coefficient R_S increases abruptly reaching its maximum. The films prepared by electron-beam evaporation consist only of the fcc phase and have a dome-like R_S dependence on film thickness.

1. Introduction

The anomalous, or extraordinary, Hall effect (EHE) still remains poorly understood although it was first discovered more than 100 years ago. The Hall effect in ferromagnetics and normal metals with magnetic dopants is usually described by the equation [1,2].

$$V_H = (\rho_H I)/d = (R_o B + R_s \mu_o M) \cdot I/d \quad (1)$$

where V_H is the Hall voltage, ρ_H is the Hall resistivity, B is the magnetic induction, M is the magnetization, I is the applied current, d is the film thickness, and R_O is the ordinary Hall coefficient which is related to the Lorenz force acting on moving charge carriers in a magnetic field. R_S is the extraordinary Hall coefficient associated with a break of the right-left symmetry during the spin-orbit scattering in magnetic materials. R_S can be much larger than R_O. This is the case of the extraordinary Hall effect (with the Hall voltage being proportional to magnetization) [3,4].

In bulk magnets it has been established, both experimentally and theoretically, that there is a direct correlation between the extraordinary Hall coefficient and longitudinal resistivity in the form $R_s \propto \rho^n$, where n depends on the predominant scattering mechanism. There are two types of carrier scattering [5,6]. The first one is skew scattering ($n=1$). It is characterized by a constant angle θ_S at which scattered carriers deviate from their initial trajectory. The other scattering type (side jump) is of quantum-mechanical nature. The result of this scattering is lateral displacement Δy of the charge trajectory in the scattering point. In this case $n=2$. Superposition of two contributions is usually presented as $R_s = a\rho + b\rho^2$, where a and b are coefficients corresponding to the skew scattering and side jump, respectively. The experimental results on EHE relation to resistivity in different ferromagnetic materials are reviewed in [7,8].

The recent interest to EHE is due to the fact that the value of this effect in ultrathin nickel [3] and FePt [9] films turned out to be 2–3 orders of magnitude larger than that of normal Hall effect and it is comparable with the Hall effect in semiconductors. A record-high value of sensitivity $S = \Delta R_H/\Delta B = 1200\ \Omega/T$ was obtained on multilayer structures $Co_{0.9}Fe_{0.1}/Pt$ [10]. One more reason of the growing interest to EHE is that this effect can be used as a simple and efficient tool to measure magnetic characteristics of thin films and magnetic objects of nanoscale sizes [11,12]. It was found that magnetization of thin nickel films can be determined by measuring their Hall resistivity [13]. EHE was observed in systems where ferromagnetic particles were embedded in dielectric [14] or different metallic matrices [9,13,15]. EHE is highly sensitive to local magnetic moments of individual nanoparticles in contrast to macroscopic magnetization of bulk magnetics. So, it is of interest to study this effect in ultrathin films and granulated ferromagnetics with the magnetic component content below the percolation threshold. The boundaries between the surrounding matrix and the ferromagnetic clusters are one of the defects on which carriers are scattered on current passing. In thin films an important factor is their surface which substantially contributes to carrier scattering as its thickness decreases [7,16].

There is a large number of works which report studies on magnetization and EHE in bulk and thin film nickel samples. The earlier among them are in [17–22]. Magnetization of thin nickel films as a function of their thickness and temperature was studied in Refs,

* Corresponding author. Tel.: +7 9150300443.
E-mail address: villev@iptm.ru (V. Levashov).

0040-6090/$ – see front matter © 2011 Elsevier B.V. All rights reserved.
doi:10.1016/j.tsf.2011.01.377

[18–21]. The lower thickness level was about 1 nm. At thicknesses less than 2 nm no film magnetization was observed. It was supposed that the deposition of nonmagnetic Ni with a hexagonal lattice could occur during the film fabrication, but no final conclusion was found. EHE in thin (less than 10 nm) Ni films was measured at room temperature [20] and in the temperature range from liquid helium to the Curie point [22]. In more recent works on EHE in thin Ni films it is worth to point out the works [8,13], where the influence of surface scattering effect on the R_S coefficient was researched in particular. Work [7] is also worth to be mentioned. It is devoted to the relation between EHE and resistivity of thin Ni films. Extremely thin films are of particular interest, because Ni film sensitivity in the field increases with the decrease of their thickness [13].

In this work, EHE in ultrathin Ni films prepared by different deposition techniques was studied in order to determine the lowest thickness level at which their field sensitivity is maximum.

2. Experiment

Samples of thin Ni films were prepared by two techniques. The first was diode radio-frequency (plasma) sputtering of a nickel target on a Z-400 installation. The working Ar pressure was 1 Pa. The target–substrate distance was 35 mm. The other technique was electron-beam evaporation on the L-560 installation, with the target-substrate distance of about 300 mm. In both cases the working chambers were evacuated with a turbomolecular pumps and the residual pressure before metal film deposition was $1 \cdot 10^{-4}$ Pa. In both cases silicon with a 0.3 μm thick silicon dioxide SiO_2 layer served as a substrate. The deposition was performed at room temperature through an aluminum foil mask with a cross-shaped aperture (the width of lines was 1 mm). The thickness of the films was checked with a profilometer and a quartz resonator. The deposition rate for Ni was 0.28 nm/s. The Hall voltage was measured in magnetic field normal to the sample plane. All experiments were performed at room temperature. Structure studies were performed using a DRON-UM-L diffractometer ($CuK_{\alpha,\beta}$ radiation at different angles of beam inclination) and JEOL JEM-100CX and JEM-2000FX microscopes at 100 and 150 kV accelerating voltages, respectively.

3. Results and discussion

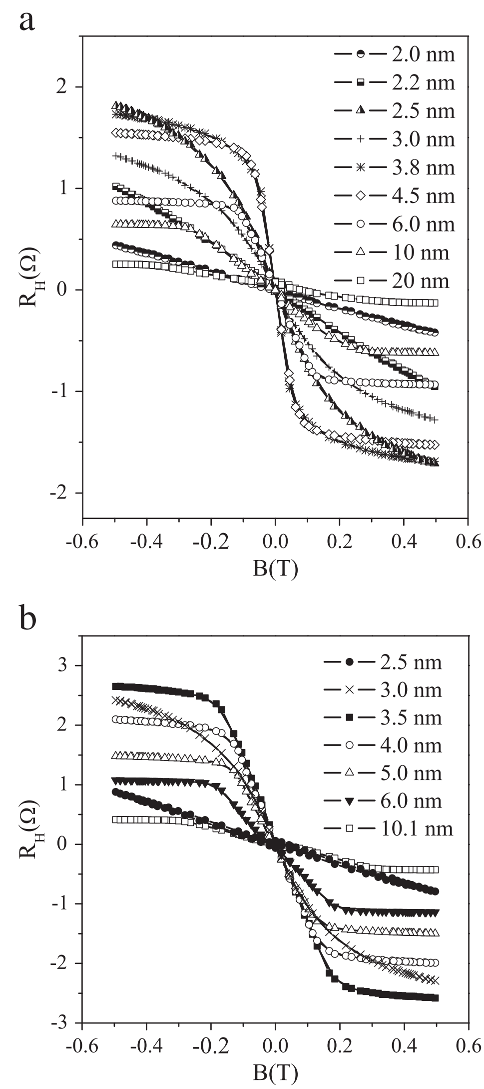

Fig. 1. Hall resistance dependence on the magnetic field for Ni films of different thickness at room temperature: a) RF-diode sputtering, b) electron-beam evaporation.

The Hall resistance dependence on the magnetic field at room temperature for Ni films of different thicknesses prepared by different techniques is shown in Fig. 1. At plasma sputtering, R_H dependence on film thickness can arbitrarily be divided into three regions. The first region—the thickness of the Ni films ranges from 4.5 to 20 nm. Both ordinary and extraordinary Hall effect (EHE) are observed at the film thickness 20 nm. The value of the extraordinary Hall effect is 20 times larger than that of the ordinary Hall effect (OHE). As the film thickness decreases down to 4.5 nm EHE arises, with its value growing the larger, the thinner becomes the film. For all films in this region R_H reaches saturation in fields higher than 0.3 T. The second region covers film thicknesses from 2.5 to 2.0 nm. As the film thickness decreases R_H decreases too and does not saturate in fields up to 0.5 T. For intermediate thicknesses 3.8 to 3.0 nm the R_H does not reach saturation either. The maximum sensitivity 22 Ω/T corresponds to the thickness of 4 nm.

For the films prepared by electron-beam evaporation (Fig. 1b), the behavior of Hall resistance as a function of magnetic field is similar to that shown in Fig. 1a. With decreasing film thickness from 10 to 3.5 nm, R_H reaches saturation in a magnetic field of around 0.3 T. At smaller thickness no saturation is observed in fields less than 0.5 T, and the R_H value drops. The maximum sensitivity 15 Ω/T corresponds to the film thickness of 3.5 nm.

Fig. 2 shows the dependences of the extraordinary Hall coefficient R_S and the resistivity ρ on the Ni film thickness obtained by different techniques. In the case of plasma sputtering (Fig. 2a), the resistivity of 2 to 2.5 nm thick films drops abruptly, then decreases stepwise at film thickness from 2.5 to 4 nm, and later by 4 to 10 nm thickness it remains practically constant and equal to ~40 $\mu\Omega \cdot$cm. For films prepared by electron-beam evaporation (Fig. 2b), the resistivity drops abruptly in the region of 2 to 3.6 nm thickness and then smoothly decreases to 30 $\mu\Omega \cdot$cm at the thickness of 10 nm. In both cases the ρ dependence on the thickness is characteristic of the process of metal film growth from an islanded structure transition to a uniform film through the formation of an infinite cluster as the percolation threshold is reached [23]. Note that precise determination of the percolation threshold of the films prepared by different techniques was not a goal of this work. Film resistance is known to drop abruptly when the percolation threshold is reached [23,24]. To the sufficient precision in our case, the percolation threshold was reached in the range 2.0–2.5 and 2.2–3.6 nm thicknesses in the films prepared by plasma sputtering and electron-beam evaporation, respectively. This is supported by the morphology of films of different thickness shown in Fig. 3.

The film morphology clearly explains their resistivity behavior. At the thickness of 1.5 nm both films consist of isolated islands. At 2.2 nm, films prepared by RF-diode sputtering are more uniform than those fabricated by electron-beam evaporation and correspondingly